Archival Report

Biological Psychiatry: GOS

Identifying Subgroups of Major Depressive Disorder Using Brain Structural Covariance Networks and Mapping of Associated Clinical and Cognitive Variables

Xiao Yang, Poornima Kumar, Lisa D. Nickerson, Yue Du, Min Wang, Yayun Chen, Tao Li, Diego A. Pizzagalli, and Xiaohong Ma

ABSTRACT

BACKGROUND: Identifying data-driven subtypes of major depressive disorder (MDD) holds promise for parsing the heterogeneity of MDD in a neurobiologically informed way. However, limited studies have used brain structural covariance networks (SCNs) for subtyping MDD.

METHODS: This study included 145 unmedicated patients with MDD and 206 demographically matched healthy control subjects, who underwent a structural magnetic resonance imaging scan and a comprehensive neurocognitive battery. Patterns of structural covariance were identified using source-based morphometry across both patients with MDD and healthy control subjects. K-means clustering algorithms were applied on dysregulated structural networks in MDD to identify potential MDD subtypes. Finally, clinical and neurocognitive measures were compared between identified subgroups to elucidate the profile of these MDD subtypes.

RESULTS: Source-based morphometry across all individuals identified 28 whole-brain SCNs that encompassed the prefrontal, anterior cingulate, and orbitofrontal cortices; basal ganglia; and cerebellar, visual, and motor regions. Compared with healthy control subjects, individuals with MDD showed lower structural network integrity in three networks including default mode, ventromedial prefrontal cortical, and salience networks. Clustering analysis revealed two MDD subtypes based on the patterns of structural network abnormalities in these three networks. Further profiling revealed that patients in subtype 1 had younger age of onset and more symptom severity as well as greater deficits in cognitive performance than patients in subtype 2.

CONCLUSIONS: Overall, we identified two MDD subtypes based on SCNs that differed in their clinical and cognitive profile. Our results represent a proof-of-concept framework for leveraging these large-scale SCNs to parse heterogeneity in MDD.

https://doi.org/10.1016/j.bpsgos.2021.04.006

Major depressive disorder (MDD) is a highly heterogeneous disorder (1). This clearly points to different MDD subtypes with potentially distinct pathophysiology. In addition, their underlying neurobiological mechanisms are unknown, posing a substantial barrier to understanding this prevalent disorder. Recently, there has been a renewed interest in utilizing data-driven approaches to identify homogeneous patient subgroups or subtypes, which is expected to lead to the development of more biologically informed, patient-specific diagnosis and treatment (2).

Research into parsing MDD heterogeneity so far has been focused on subtyping based on symptoms or clinical features, genetics, medication response, and neurotransmitter distribution (2–4). Recently, biotypes identified using brain-based measures have shed some light on parsing the heterogeneity of depression, and these biotypes can identify groups of patients with different disease course or treatment response. One such study used resting-state connectivity biomarkers to group 711 participants with depression into four depression biotypes that were differentially responsive to transcranial magnetic stimulation therapy (5). Even though resting-state connectivity measures have been shown to be critical for these approaches (6–8), very few studies have utilized widely available structural data to identify subgroups.

We utilize a novel technique known as source-based morphometry (SBM), which implements independent component analysis (ICA) to study morphometric measures of gray matter (GM) structural covariance networks (SCNs) across participants (9–11). Structural covariance might be a valuable tool for investigating the topological organization of the brain (11,12). SCNs are based on the observation that interindividual differences in the structure of a GM region often covary with interindividual differences in the structure of other GM regions within networks of brain regions that fluctuate in morphometric

ISSN: 2667-1743

properties across participants (13). In addition, SCNs partially overlap functional brain networks that subserve behavioral and cognitive functions, although structural covariance is thought to arise from coordinated development and synchronized maturation between brain regions as well as white matter and functional connectivity between brain regions. Therefore, SCNs may be a valuable tool for investigating the topological organization of the brain and for investigating aberrant connectivity and brain network organization in psychiatric disorders (13–15). In addition, structural data are much more robust and reliable because they change very slowly over years, and morphometric covariance could provide a new and robust way to study heterogeneity in psychopathology, especially in MDD. In addition, by reflecting the distributed nature of neural activity that underlies disorders, SBM has the potential to provide greater insight into disease progression and pathology, and it might be a better measure to parse individuals than a focal approach. This provides not only complementary information to other connectivity approaches but also possible insights into more stable (e.g., maturational or trait-like) structural features and comprehensive characterization of network-level brain features (14).

Previous studies that relied on this method in patients with schizophrenia identified the most significant source of schizophrenia-related GM changes in the basal ganglia, parietal lobe, and occipital lobe (9). Interestingly, these changes did not emerge from traditional voxel-based morphometry (VBM) analysis. These findings suggest that SBM is a multivariate alternative to VBM, with wide applicability to studying changes in brain structure (9). For example, when compared with healthy control (HC) subjects, the whole-brain structural network of patients with Alzheimer's disease was found to be more segregated and less integrated (15,16). In addition, the SBM procedure identified patterns of structural covariance that are consistent with spatial patterns of functionally correlated brain regions. There was substantial spatial overlap between identified component and the regions of the default mode network (DMN) (17–19).

Structural covariance patterns of the visual cortex, anterior insula, and parietal cortex as well as bilateral temporal and prefrontal cortices (20–22) have been shown to be related to functional networks (19,23). These observations are generally consistent with evidence of substantial overlap between spatial patterns of structural networks and functional connectivity patterns observed using resting-state functional magnetic resonance imaging (24). Studies that have investigated structural connectivity in MDD have primarily relied on a seed-based approach to identify structural connectivity of a priori regions of interest (25), therefore missing the critical exploration into the whole-brain network-level structural deficits in MDD.

To address limitations of previous studies, we had two main objectives in this study. First, we utilized the SBM approach to contrast whole-brain structural GM covariance networks between HC subjects (n = 206) and individuals with MDD (n = 145) and identify networks that are altered in patients with MDD. Second, based on the alterations of SCNs in MDD, we aimed to identify potential biological subtypes of depression based on structural covariance patterns and to evaluate the clinical and neurocognitive differences between the identified subgroups of individuals with MDD using exploratory analyses.

METHODS AND MATERIALS

Participants

A total of 206 HC subjects and 145 unmedicated individuals with MDD participated in this study. All participants were Han Chinese between the ages of 18 and 55 years and provided written informed consent to a protocol approved by the ethics committee of West China Hospital, Sichuan University. This study was conducted in accordance with the Declaration of Helsinki (for details, see the Supplement). All individuals were evaluated by two trained psychiatrists (XHM and YD) using the Structured Clinical Interview for DSM-IV (26) to confirm study eligibility; participants with MDD had to be in a current depressive episode according to the Structured Clinical Interview for DSM-IV. In addition, individuals with MDD were also assessed using the 17-item Hamilton Depression Rating Scale (HDRS) (27) and were excluded if they scored less than 17 on the HDRS. Patients were recruited by referrals from psychiatrists, and healthy volunteers were recruited from the local community. All patients with MDD were currently unmedicated. Eighty-six of the 145 patients (59.3%) were in their first episode and drug naïve. Remaining participants had not taken antidepressants for at least 3 months before the study visit.

Neuropsychological Assessments

The short version of the Wechsler Adult Intelligence Scale–Revised in China was administered to assess general intelligence (28). Five subsets of the computerized Cambridge Neurocognitive Test Automated Battery were included in this study that have been shown to be sensitive and validated for studying cognition in depression. These tasks included the Delayed Matching to Sample (DMS), Stockings of Cambridge, Rapid Visual Information Processing (RVP), Spatial Working Memory, and Pattern Recognition Memory, which assess visuospatial working memory and executive function (for details, see the Supplement).

Image Acquisition

Structural data were collected using a Philips 3T scanner (Philips, Amsterdam, the Netherlands) with an eight-channel phased-array head coil. High-resolution T1-weighted images were obtained using a magnetization prepared rapid acquisition gradient-echo sequence. Imaging parameters were as follows: repetition time = 8.4 ms; echo time = 3.8 ms; flip angle = 7°; acquisition matrix = 256 × 256; field of view = 256 × 256 mm^2; voxel size = 1 × 1 × 1 mm^3; number of slices = 188.

Voxel-Based Morphometry

Structural data were analyzed with FSL-VBM (29), an optimized VBM protocol (30) in FSL (31). First, structural images were brain extracted and GM segmented before being registered to the MNI152 standard space using nonlinear registration (32). The resulting images were averaged and flipped along the x-axis to create a left-right symmetric, study-specific GM template. Second, all native GM images were nonlinearly

registered to this study-specific template and modulated to correct for local expansion (or contraction) due to the nonlinear component of the spatial transformation. The modulated GM images were then smoothed with an isotropic Gaussian kernel with a sigma of 3 mm (full width at half maximum = 2.35 × 3 mm = 7.05 mm). A four-dimensional subject series of these smoothed GM images was created by concatenating all subjects' spatial maps, which was utilized as input for subsequent analyses (29,31–33).

Estimating SCNs Using MELODIC ICA

MELODIC was used to decompose the four-dimensional subject series of GM maps (generated from the VBM analysis) into independent components (ICs) that reflect sources of shared spatial covariance. The number of components (model order) was selected as 30, which gave spatial patterns consistent with previous studies probing resting-state and SBM networks (15,18,32–35). To ensure stable convergence of the ICA (i.e., to ensure that the resulting ICs were consistent), we estimated group ICA maps with different numbers of components: 20, 25, 30, 35, and 40. Different model orders yielded similar results. This was consistent with the previous resting-state network analyses by author LDN, who had previously demonstrated reproducibility of brain networks using model orders of 20 and 70 (36). Similarly, in this study, we found that components identified using a model order of 30 were robust and stable and provided clearer separation of signal and noisy components. All group independent component analysis (GICA) results were first assessed independently as to which dimensionality gave the best separation of signals from noise by authors PK and XY, and a final decision was made by LDN, who provided the expert guidance for the final selection.

Selection of A Priori SCNs. The spatial composition of each component at model order = 30 was then evaluated (Figure S1). Components comprising possible artifacts or mixed tissue sources such as sharp edges, especially near the boundary of the brain, or appearing primarily in regions that do not contain GM (e.g., white matter or ventricles) or significant spatial overlap with ventricles, WM, large vasculature, and the brainstem (20,34,35), were labeled as artifacts. Based on these criteria, we identified two components (IC #23 and IC #28) (Figure S1) as artifacts. From the remaining 28 components, we selected components that reflected cortical networks (e.g., prefrontal, anterior cingulate, and posterior cingulate cortices) and basal ganglia as the structural and functional properties of these regions have been identified by our previous work and by others to be involved in emotion and cognitive function in MDD (20,36,37). To this end, cortical and basal ganglia networks of interest were identified by visual inspection as those corresponding to previously reported SCNs (18,38–41). There is also a spatial correspondence between SCNs and resting-state networks, as can be seen in Figure 7 of Gupta for several networks, including some of our networks of interest (38). Therefore, we also identified via visual inspection SCNs that resembled resting-state networks implicated in emotion and cognitive function (34,35) and in which prefrontal, anterior cingulate, and posterior cingulate cortices and basal ganglia are key nodes. In addition, we observed some small subregions in our regions of interest that showed connectivity with primary sensory motor networks. However, for this study, we focused on networks implicated in emotion/cognition. The independent component maps were then thresholded to a z score of ± 3 (which was the average threshold determined by applying a Gaussian-gamma mixture model to each component's distribution of voxel values to determine the threshold corresponding to $p = .6$, which provides a threshold corresponding to a voxel value having a higher probability of being in the signal than in the noise). Next, each IC was normalized to maximum value of 1 by dividing each component by its maximum z score to account for differences in the scale of the spatial maps. Finally, as the subject series for each component output from the ICA is obtained with respect to the principal component analysis–reduced data that are fed into the ICA for unmixing, these loadings are not relevant to the analyses. Therefore, the loadings (strength of the network) corresponding to each normalized IC of each participant was extracted by doing a multivariate spatial regression of the set of 10 ICs against the four-dimensional GM subject series.

Statistical Analysis

All analyses were conducted in SPSS (version 24.0; IBM Corp., Armonk, NY) and MATLAB (version 2018a; The MathWorks, Inc., Natick, MA).

Demographics. Student's t and χ^2 tests were used to compare demographics variables including age, sex, education, and IQ.

Group Differences in the Strength of A Priori SCNs. Analyses of covariance (ANCOVAs) were conducted to identify group differences in the strength of the a priori SCNs between MDD and HC groups. Bonferroni correction for multiple comparisons were applied.

Identification of MDD Subgroups Using SCNs With K-Means Clustering. K-means clustering was applied to loadings for SCNs of interest that showed group differences between MDD and HC to identify MDD subgroups. K-means clustering designates clusters of participants with similar patterns of structural covariance alterations (42). The optimal cluster number (evaluated for a range of 2–6) was determined using the silhouette coefficient (43), Calinski-Harabasz index (44), and gap statistic (45,46), with additional details provided in the Supplement.

Cluster Profiling of MDD Subtypes. Based on the MDD subgroups we obtained from clustering analysis, ANCOVAs were conducted to assess differences in clinical variables and neurocognition performance among depression subgroups and HC, while controlling for age, sex, and education years as covariates.

RESULTS

Demographics

Compared with HC, individuals with MDD reported fewer education years ($p < .001$), but no differences in age or sex were observed. Table 1 summarizes demographic and clinical characteristics of MDD and HC participants.

Selection of SCNs

Ten components were selected from 28 ICs based on their spatial overlap with brain regions commonly involved in emotion and cognitive function in depression (20,37) (see Table 2 and Figure 1).

Group Differences in the Strength of SC Differences Between MDD and HC

ANCOVAs conducted with age, sex, and education years as covariates of no interest (Table 2) showed that relative to HC subjects, individuals with MDD had lower structural network integrity in structural networks corresponding to the anterior DMN ($F_{1,346} = 9.33$, $p = .002$, $\eta^2 = 0.026$), ventral medial prefrontal cortex (vmPFC) ($F_{1,346} = 12.94$, $p < .001$, $\eta^2 = 0.036$), and salience network ($F_{1,346} = 18.64$, $p < .001$, $\eta^2 = 0.051$) (Table 2), significant after correcting for multiple comparisons.

Identification of MDD Subgroups Using SCNs

To identify MDD subgroups, we applied K-means clustering to the loadings for the SCNs that showed a significant group difference between MDD and HC (i.e., vmPFC, anterior DMN, and salience network). We evaluated the optimal number of clusters between 2 and 6 using three criteria. All three cluster validation metrics resulted with 2 as the optimal number of clusters. Our clustering result achieved the maximum for the silhouette score (0.482), Calinski-Harabasz index (78), and gap statistic (0.67) when the cluster number was 2. The results of K-means clustering are illustrated in Figure 2.

Resampling 5000 times with 80% of the sample randomly selected (with replacement) as the training set showed a two-cluster solution 86% of the time with 98% of participants grouped into the same cluster with approximately 99% probability. Three participants were found to have inconsistent assignment between the two clusters.

Cluster Profiling of MDD Subtypes

Eighty-six patients (59.31%) were assigned to subgroup 1, and 59 patients (40.69%) to subgroup 2.

Subgroup Differences in Demographics and Clinical Symptoms

Participants in subgroup 2 were older than those in subgroup 1 ($p < .001$) and HC subjects ($p = .002$). Compared with patients in subgroup 2, those in subgroup 1 had a higher HDRS score ($p = .036$) and a younger age of onset ($p < .001$) (controlled for total duration). The two depression subgroups did not differ in their total illness duration, current illness duration, and presence of suicidal behavior or suicidal ideation (Table 3).

Subgroup Differences in Neurocognitive Tests

All of the following analyses were conducted with age, sex, and education years as covariates of no interest (Table 4 and Figure 3; Table S3).

DMS Task—Accuracy (Percent Correct). A one-way group (subgroup 1/subgroup 2/HC subjects) ANCOVA on percent correct revealed a significant main effect of group ($F_{2,345} = 7.97$, $p < .001$, $\eta^2 = 0.044$). Post hoc pairwise comparisons clarified that subgroup 1 had significantly lower accuracy than HC ($p < .001$) and a trend difference when compared with subgroup 2 ($p = .1$). However, subgroup 2 did

Table 1. Participant Demographics and Clinical Characteristics

Characteristics	MDD, $n = 145$	HC, $n = 206$	t/χ^2	p Value
Age, Years	28.12 ± 9.27	27.67 ± 8.76	0.46	.649
Sex, Male/Female, n	50/95	74/132	0.08	.781
Education, Years	13.34 ± 3.31	14.73 ± 3.57	−3.68	<.001[a]
Full IQ	104.80 ± 16.02	111.83 ± 14.23	4.03	<.001
HDRS Score	22.74 ± 4.08	–	–	–
GAF	51.76 ± 8.11	–	–	–
Age of Onset	26.24 ± 9.10			
Number of Episodes	1.96 ± 2.38	–	–	–
Total Disease Duration, Months	31.77 ± 51.24			
Total Disease Burden ([Total Illness Duration in Years/Current Age] × 100%)	9.19 ± 13.24	–	–	–
Current Disease Duration, Months	4.69 ± 4.31	–	–	–
Presence of Suicidal Thoughts, No/Yes, n	51/85	–	–	–
Presence of Suicidal Behavior, No/Yes, n	117/19	–	–	–
First Episode, No/Yes, n	52/86	–	–	–

Values are presented as mean ± SD unless indicated otherwise. Sample size differs due to missing data. Missing data: IQ (MDD: 23; HC: 21); HDRS (MDD: 5); GAF (MDD: 14); age of onset (MDD: 9); number of episodes (MDD: 7); total disease burden (MDD: 8); current disease burden (MDD: 8); suicidal ideation, suicidal behavior (MDD: 9); first episode (MDD: 7).

GAF, Global Assessment of Functioning; HC, healthy control; HDRS, Hamilton Depression Rating Scale; MDD, major depressive disorder.

[a]$p < .05$.

Table 2. Structural Covariance Network Differences Between Patients With MDD and HC Subjects

Structural Covariance Components	Regions of Each Component	MDD	HC	F^a	*p* Value
IC1, Basal Ganglia—Limbic Network	Basal ganglia including bilateral putamen, caudate, nucleus accumbens, pallidum; limbic including bilateral thalamus, amygdala, anterior hippocampus	0.110 ± 0.101	0.121 ± 0.118	1.146	.285
IC2, Medial OFC—Limbic Network	Bilateral medial orbital frontal cortex, limbic including bilateral thalamus, posterior hippocampus, habenula, amygdala	0.264 ± 0.072	0.272 ± 0.071	1.031	.311
IC3, Precuneus	Bilateral precuneus cortex, superior parietal gyrus, posterior cingulate cortex	0.368 ± 0.126	0.380 ± 0.115	2.415	.121
IC4, DMN	Bilateral precuneus cortex, lingual gyrus, posterior cingulate cortex, anterior dorsal cingulate gyrus	0.298 ± 0.078	0.322 ± 0.081	9.325	.002[b]
IC5, vmPFC	Bilateral ventral medial prefrontal cortex, lateral OFC, rostral anterior cingulate gyrus, anterior insular cortex	0.409 ± 0.097	0.444 ± 0.088	12.935	<.001[b]
IC6, dACC	Bilateral dorsal anterior cingulate cortex, left dorsal lateral prefrontal gyrus, bilateral medial orbital frontal cortex	0.149 ± 0.094	0.163 ± 0.103	2.958	.086
IC7, Operculum	Bilateral operculum cortex, inferior frontal gyrus, anterior insula cortex, lateral orbital frontal cortex	0.311 ± 0.077	0.320 ± 0.079	0.651	.420
IC8, Cingulo-opercular	Bilateral anterior insula cortex, frontal pole, posterior cingulate gyrus, operculum cortex, paracingulate gyrus, dorsal anterior cingulate gyrus, precuneus	0.546 ± 0.071	0.556 ± 0.074	2.828	.094
IC9, SN	Bilateral paracingulate gyrus, dorsal lateral prefrontal gyrus, dorsal anterior cingulate gyrus	0.385 ± 0.058	0.407 ± 0.062	18.635	<.001[b]
IC10, Middle Frontal	Middle frontal gyrus, paracingulate gyrus, anterior cingulate gyrus	0.276 ± 0.060	0.280 ± 0.069	0.373	.542

Values are presented as mean ± SD. Components are named based on the overlap of the spatial extent of these components with the corresponding resting-state networks. ICs are listed in the order of the cluster size.

dACC, dorsal anterior cingulate cortex; DMN, default mode network; HC, healthy control; IC, independent component; MDD, major depressive disorder; OFC, orbitofrontal cortex; SN, salience network; vmPFC, ventral medial prefrontal cortex.

[a]*df* = 346.

[b]*p* value was adjusted for Bonferroni correction ($p < .05/10 = .005$). Age, sex, and education years entered as covariates.

not differ from HC ($p = .12$). These results suggest that although both subgroups had overall impairments, subgroup 1 was numerically more impaired than subgroup 2.

DMS Task—Mean Correct Latency. No significant results were obtained.

Stockings of Cambridge Task—Mean Moves and Percent Correct. No significant results were obtained.

RVP Task—A Prime (Sensitivity). A one-way group (subgroup 1/subgroup 2/HC subjects) ANCOVA of A prime revealed a significant main effect of group ($F_{2,345} = 4.23$, $p = .015$, $\eta^2 = 0.024$). Follow-up of the main effect of group showed that subgroup 1 had a significantly lower sensitivity than HC subjects ($p = .006$) and subgroup 2 ($p = .025$).

RVP Task—B Double Prime. No significant results were obtained.

RVP Task—Mean Correct Latency. A one-way group (subgroup 1/subgroup 2/HC subjects) ANCOVA on mean correct latency revealed a significant main effect of group ($F_{2,345} = 3.73$, $p = .025$, $\eta^2 = 0.021$). Post hoc analyses

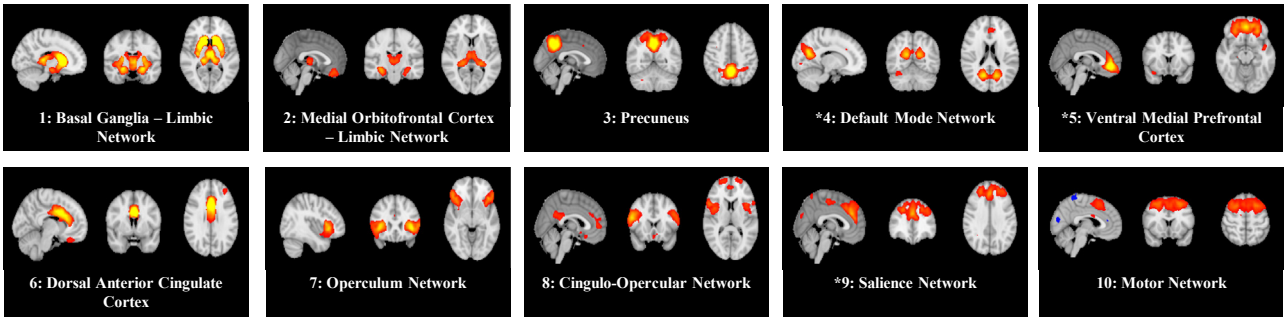

Figure 1. Ten selected structural covariance networks across healthy individuals and patients with depression. *In comparison with healthy control subjects, patients with major depressive disorder had lower structural network integrity in the default mode network (independent component #4), ventromedial prefrontal cortex (independent component #5), and salience network (independent component #9).

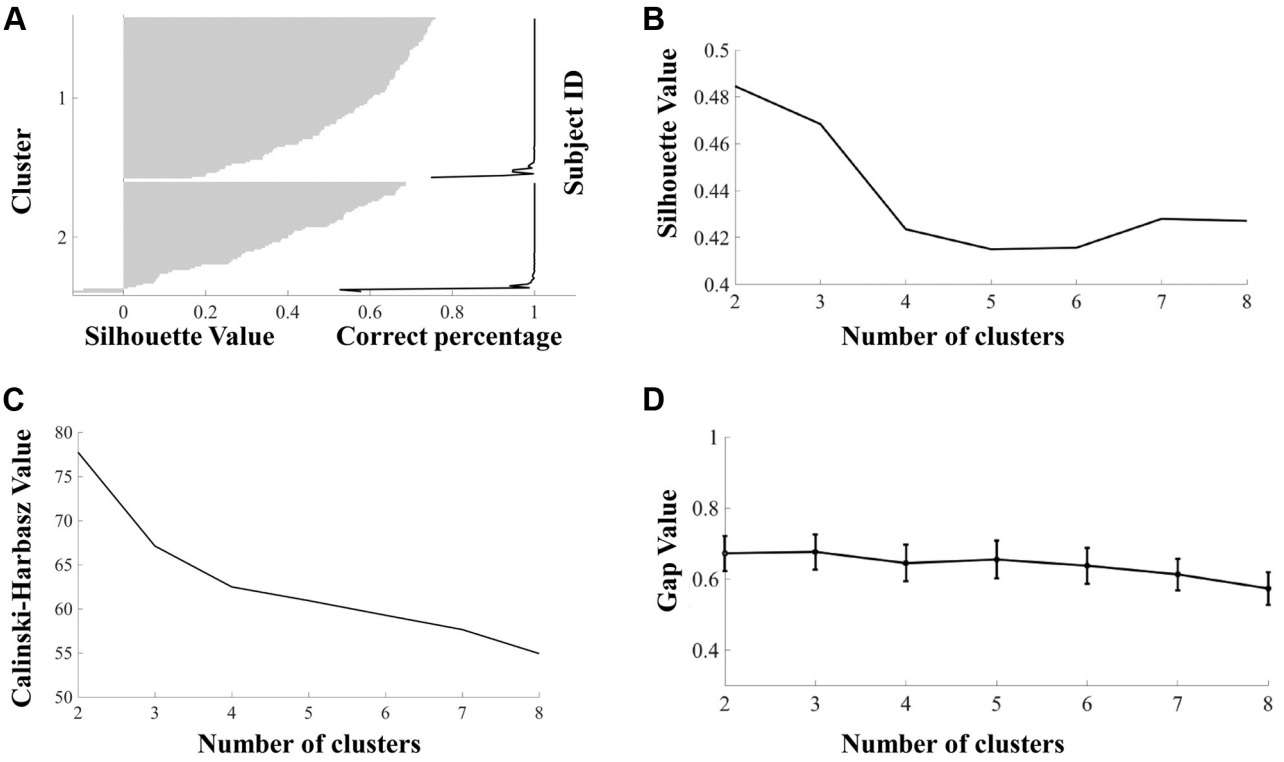

Figure 2. Validation of clusters. Optimal number of clusters was determined to be 2 based on the silhouette score of 0.482 **(A, B)**, Calinski-Harabasz score of 78 **(C)**, and gap statistic of 0.67 **(D)**. Eighty-six patients (59.31%) were assigned to subgroup 1, and 59 patients (40.69%) were assigned to subgroup 2. Resampling 5000 times with 80% of the sample randomly selected (with replacement) as the training set showed 98% of participants grouped into the same cluster with approximately 99% probability **(A)**.

clarified that subgroup 1 had an increased mean latency than HC (p = .008) and a trend when compared with subgroup 2 (p = .064), suggesting that subgroup 1 was slower overall.

Spatial Working Memory Task—Total Errors and Strategy. No significant results were obtained.

Pattern Recognition Memory Task—Accuracy (Percent Correct). A one-way group (subgroup 1/subgroup 2/HC subjects) ANCOVA on percent correct revealed a significant main effect of group ($F_{2,345}$ = 3.02, p = .05, η^2 = 0.017). Post hoc analyses showed that subgroup 1 had significantly lower accuracy than HC subjects (p = .015).

Pattern Recognition Memory Task—Mean Correct Latency. No significant results were obtained.

Overall Cambridge Neurocognitive Test Automated Battery Summary. Overall, our exploratory results suggest that subgroup 1 exhibited greater impairments than subgroup 2 across different domains as measured by these tasks. However, when corrected for multiple comparisons, only the accuracy on the DMS task survived. More details about Cambridge Neurocognitive Test Automated Battery are presented in the Supplement.

DISCUSSION

The main goal of this study was to utilize whole-brain structural GM covariance networks estimated by SBM to identify potential neural subtypes of depression based on changes of structural patterns. Our secondary exploratory goal was to evaluate the clinical and neurocognitive differences between the identified MDD subgroups.

To this end, we identified 28 whole-brain SCNs that encompassed the prefrontal, anterior cingulate, and orbitofrontal cortices; basal ganglia; and cerebellar, visual, and motor regions using SBM analyses across both HC and MDD individuals. Of the 10 selected networks involved in emotion- and cognition-related function, we found that individuals with MDD had lower structural covariance in three SCNs: DMN, vmPFC network, and salience network, which have been consistently reported to be impaired in MDD (41). Next, using a neuroimaging data-driven approach combined with K-means clustering techniques, we identified two depression biotypes associated with distinct clinical and neurocognitive profiles based on the

Table 3. Demographic and Clinical Characteristics of Patient Subgroups and HCs

Characteristics	Subgroup 1, n = 86	Subgroup 2, n = 59	HC, n = 206	Statistics	p Value	Post Hoc p1, p2, p3
Age, Years, Mean ± SD	25.65 ± 6.62	31.71 ± 11.26	27.67 ± 8.76	F = 8.454	.000[a]	p1: 0.073, p2: 0.002, p3: 0.000
Sex, Male/Female, n	30/56	20/39	74/132	$\chi^2_{1,350}$ = 0.092	.955	–
Education, Years, Mean ± SD	13.65 ± 3.05	12.90 ± 3.64	14.73 ± 3.57	F = 7.620	.001[a]	p1: 0.016, p2: 0.000, p3: 0.199
Full Scale IQ	104.73 ± 15.90	104.91 ± 16.43	111.83 ± 14.23	F = 8.092	<.001	p1: <0.001, p2: 0.007 p3: 0.952
HDRS, Mean ± SD	23.33 ± 4.31	21.86 ± 3.57	–	t = 2.123	.036	–
GAF, Mean ± SD	51.27 ± 7.72	52.54 ± 8.74	–	t = −0.868	.387	–
Age of Onset, Years, Mean ± SD	23.63 ± 6.99	30.20 ± 10.46	–	t = −4.392	.000	–
Age of Onset, Years, Control for Total Duration	23.63 ± 6.99	30.20 ± 10.46		F = 21.762	.000	–
Number of Episodes, Mean ± SD	1.93 ± 2.42	2.02 ± 2.35	–	t = −0.217	.828	–
Total Illness Duration, Months	30.13 ± 47.03	34.20 ± 57.32	–	t = −0.454	.651	–
Total Disease Burden, ([Total Illness Duration in Years/ Current Age] × 100%)	9.71 ± 13.99	8.27 ± 12.03	–	t = 0.622	.535	–
Current Illness Duration, Months	4.72 ± 4.13	4.65 ± 4.596	–	t = 0.081	.935	–
Presence of Suicidal Thoughts, No/Yes	32.93%/67.07%	44.44%/55.56%	–	$\chi^2_{1,136}$ = 1.843	.175	–
Presence of Suicidal Behavior, No/Yes	84.15%/15.85%	88.89%/11.11%	–	$\chi^2_{1,136}$ = 0.609	.435	–
First Episode, No/Yes	37.35%/62.65%	38.18%/61.82%	–	$\chi^2_{1,137}$ = 0.010	.921	–

Values are presented as mean ± SD unless indicated otherwise. p1: subgroup 1 vs. HC group; p2: subgroup 2 vs. HC group; p3: subgroup 1 vs. subgroup 2. Sample size differs due to missing data. Missing data: GAF (S1: 5; S2: 9); age of onset, suicidal ideation, suicidal behavior (S1: 4; S2: 5); total duration (S1: 4; S2: 5); current illness duration (S1: 5; S2: 4); number of episodes (S1: 3; S2: 4); IQ (HC: 22; S1: 8; S2: 16).

GAF, Global Assessment of Functioning; HC, healthy control; HDRS, Hamilton Depression Rating Scale.

[a]$p < .05$

three SCNs (DMN, vmPFC network, and salience network). Specifically, we found that subgroup 1 had increased MDD severity, a younger age of onset of their first MDD episode, and increased cognitive impairments when compared with subgroup 2.

Large-scale covariance of GM morphometric measures has been consistently reported in neuroimaging studies (47). Brain regions that grow together at the same rate over the course of years in the same individual are expected to demonstrate strong structural covariance across individuals (47–50). The

Table 4. Comparison of All Neurocognitive Tests Between Patient Subgroups and HC Subjects

Task	Measure	Subgroup 1	Subgroup 2	HC	Levels	Post Hoc p1, p2, p3
DMS	PC	84.63 ± 9.59	84.63 ± 11.69	88.73 ± 7.37	$F_{2,345}$ = 7.97, $p < .001$[a]	p1: 0.000, p2: 0.120, p3: 0.105
	MCL	3715.09 ± 997.87	3785.25 ± 1065.93	3599.50 ± 901.41	$F_{2,345}$ = 0.71, p = .493	–
SOC	MM	4.43 ± 0.69	4.61 ± 0.67	4.31 ± 0.62	$F_{2,345}$ = 2.67, p = .070	–
	PS	7.59 ± 2.41	7.82 ± 1.85	8.18 ± 2.20	$F_{2,345}$ = 2.29, p = .103	–
RVP	A Prime	0.89 ± 0.05	0.91 ± 0.05	0.92 ± 0.05	$F_{2,345}$ = 4.23, p = .015	p1: 0.006, p2: 0.849, p3: 0.025
	B_DP	0.94 ± 0.06	0.93 ± 0.07	0.93 ± 0.05	$F_{2,345}$ = 0.39, p = .676	–
	MCL	424.96 ± 79.41	417.62 ± 89.70	400.99 ± 71.74	$F_{2,345}$ = 3.73, p = .025	p1: 0.008, p2: 0.842, p3: 0.064
SWM	TE	27.20 ± 15.96	27.88 ± 18.74	22.37 ± 19.35	$F_{2,345}$ = 2.07, p = .127	–
	Stra	34.01 ± 4.71	33.78 ± 4.93	32.57 ± 5.22	$F_{2,345}$ = 2.82, p = .061	–
PRM	PC	171.40 ± 16.39	168.92 ± 18.74	175.58 ± 17.71	$F_{2,345}$ = 3.02, p = .050	p1: 0.015, p2: 0.430, p3: 0.245
	MCL	4245.78 ± 1133.78	4423.63 ± 958.26	4070.12 ± 868.14	$F_{2,345}$ = 1.59, p = .206	–

Values are presented as mean ± SD. p1: subgroup 1 vs. HC group; p2: subgroup 2 vs. HC group; p3: subgroup 1 vs. subgroup 2.

A Prime, signal detection measure of sensitivity to the target, regardless of response tendency (range 0.00 to 1.00; bad to good); B_DP, B double prime, signal detection measure of the strength of trace required to elicit a response (range −1.00 to 1.00); DMS, Delayed Matching to Sample; MCL, mean correct latency; MM, mean moves in all trials; PC, percent correct; PRM, Pattern Recognition Memory; PS, problems solved in minimum moves; RVP, Rapid Visual Information Processing; SOC, Stockings of Cambridge; Stra, Strategy, a high score represents poor use of this strategy and a low score equates to effective use; SWM, Spatial Working Memory; TE, total errors.

[a]Corrected for multiple comparisons using Bonferroni correction (p = .05/11 = .0045).

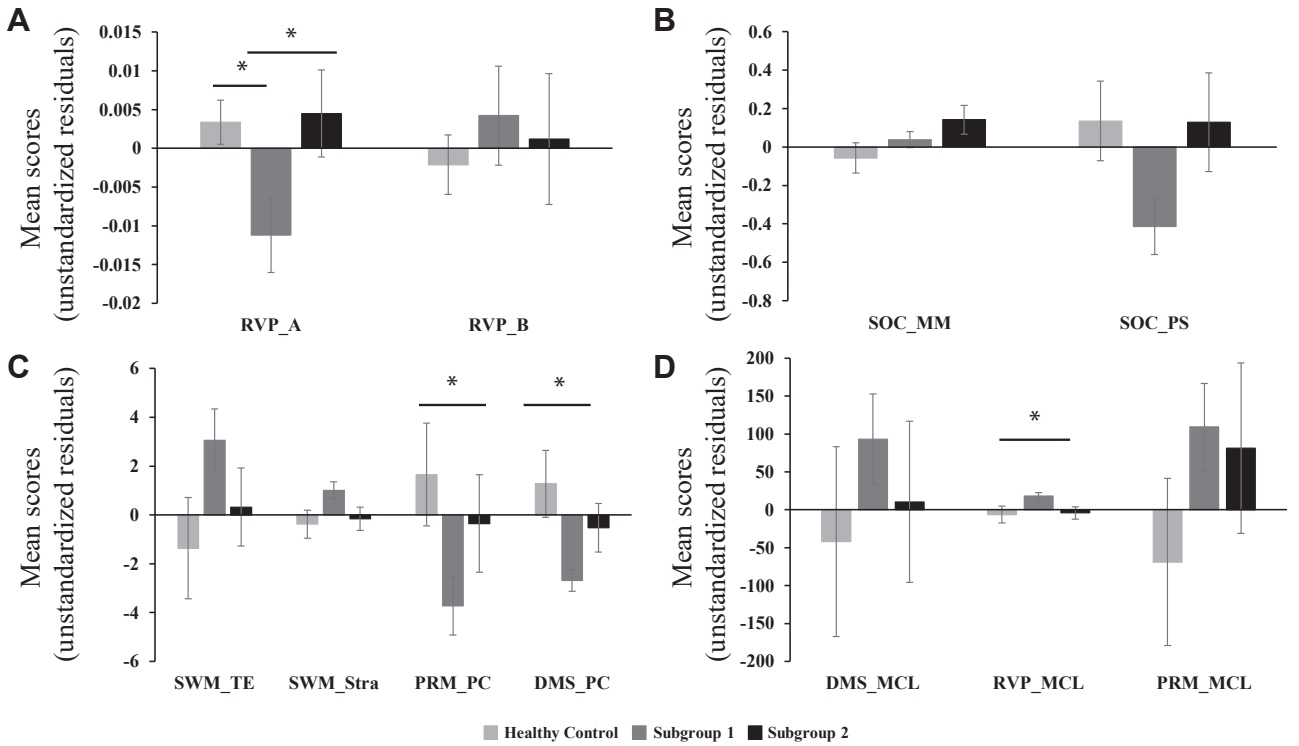

Figure 3. Major depressive disorder subgroups and healthy control group differences in neurocognitive tests. **(A)** Rapid Visual Information Processing (RVP) task; **(B)** Stockings of Cambridge (SOC) (mean moves [MM] and problems solved in minimum moves [PS]); **(C)** Spatial Working Memory (SWM) (total errors [TE] and strategy [Stra]), Pattern Recognition Memory (PRM) (percent correct [PC]), Delayed Matching to Sample (DMS) (PC); **(D)** Mean correct latency (MCL) of DMS, RVP, and PRM tasks. All analyses were conducted with age, sex, and education years as covariates of no interest. Unstandardized residuals are plotted in the figure. *$p < .05$.

existence of such networks has been recognized for over a decade. While SCNs are not direct reflections of functional connectivity or indeed structural connectivity, SCNs have been shown to some extent to correspond with functional and structural connectivity (51,52). Consistent with this and other previous studies, we found significant spatial overlap between our SCNs and reported functional connectivity networks (20,21,37,53,54). For example, the basal ganglia, vmPFC, and salience and precuneus networks had spatial patterns similar to those of functional connectivity networks reported in other studies (20,21). GM is the neuroanatomical basis of neuronal activity; thus, structural covariance measured by GM density is also possibly associated with functional correlations. The study by Seeley *et al.* discovered a striking convergence between intrinsic functional connectivity and SC, supporting the idea that functionally correlated brain regions should show correlated GM density in HC (37,55).

All three networks found to be impaired in MDD when compared with HC subjects encompassed the cingulate and prefrontal cortices (SC 1: DMN; SC 2: vmPFC; SC 3: salience network). Supporting our findings, a recent study reported anatomical covariance impairments in these networks in unmedicated MDD (56). Although studies investigating anatomical covariance are scarce, functional connectivity alterations in these networks have been commonly reported and form the basis of several neurocognitive models of depression (41,57–59).

Because of the self-referential processes attributed to the DMN (60), this network has received much attention and has been most consistently related to MDD (61). Previous findings suggest that depression is characterized by increased recruitment of regions within the DMN (62), and those abnormalities have been associated with severity (63) and length (64) of the depressive episode. In addition, the vmPFC has been shown to be significantly impaired in MDD. Postmortem studies have described reductions in GM in the vmPFC of patients with MDD, which were associated with a reduction in glia without an equivalent loss of neurons (65). The salience network–related brain regions were found to be involved in cognition, action, inhibitory control, emotion processing (34,63,66), and capturing and orienting to salient external stimuli (53). Our results of impaired structural covariance in these networks complement these functional connectivity studies (67). Together, our results stemming from a structural covariance approach further identified that these core neurocognitive networks are affected in depression.

One of the major obstacles to understanding the pathophysiology of depression is the clinical and biological heterogeneity inherent in this disorder. SCNs have been observed to be robust and highly heritable (68) and to show systematic

differences with age and disease status (15,55,69,70). SCNs can therefore provide insight into disease progression and pathology, and these networks might be a better measure to parse individuals (14). To this end, we utilized a K-means algorithm to identify two MDD subgroups based on the three SCNs that were shown to be impaired in participants with MDD. We observed that subgroups 1 and 2 had different clinical profiles: subgroup 1 had higher depression severity (as assessed by HDRS) and younger age of onset than subgroup 2.

In addition to clinical differences, exploratory analyses revealed a differential cognitive performance profile. Specifically, we found that subgroup 1 also had more pronounced cognitive impairments as shown by lower accuracy, higher probability of errors, and longer reaction times across different cognitive domains. Of note, MDD has been associated with neurocognitive abnormalities, including in tasks probing attention, working memory, and executive function, and impaired cognition has been estimated to occur in around two-thirds of patients with depression (71,72). Cognitive impairment is a significant determinant of social and occupational function in psychiatric disease, and impaired ability to think, concentrate, or make a decision is a DSM-5 diagnostic criterion for MDD (73). Patients with cognitive impairment may contribute to poorer treatment adherence and outcomes (74). Recent studies have shown that cognitive performance predicted clinical symptoms and antidepressant treatment response in depression (75). While the recovery of the cognitive deficits after clinical remission from depression may be associated with subtypes of MDD (76), several other novel agents may be repurposed as cognitive enhancers for MDD treatment for those patients who continue to experience significant cognitive impairment (77). The clinical profile difference, specifically with age of onset, is potentially significant because age of onset is often observed to be a source of heterogeneity (78) with greater chronicity and genetic liability associated with the illness (79). Furthermore, the subgroup with earlier age of onset was the one showing greater cognitive impairments, highlighting the influence of disease burden on cognition/behavior.

Even though these results warrant replication, we believe that SCNs can provide a reliable measure for identifying biotypes and can be leveraged to develop classifiers. The present network analysis of structural data is analogous to that of functional data. However, structural data are much more robust and reliable because they change very slowly over years (9). In addition, morphometric covariance could provide a new and robust way of estimating the linked patterns of interregional similarity and anatomical connectivity within an individual human brain. Therefore, structural network analysis holds great promise in many areas of neuroscience (14).

There are several limitations that should be emphasized. First, we conducted clustering on the three networks that were overall impaired in the MDD group, as we were interested in identifying subgroups that show MDD-related impairments. Second, when corrected for multiple comparisons, only the accuracy on the DMS task survived; therefore, these results should be taken as exploratory, and replication is warranted. Third, only the HDRS scale was used to assess depression severity, which limited our ability to evaluate whether subgroups differed in other MDD phenotypes (e.g., anhedonia and anxiety). Finally, although the current results highlighted the promise of utilizing SCNs to identify subtypes of MDD and its associated clinical and cognitive profile differences, we did not have an independent sample to confirm generalizability and replicability of findings.

ACKNOWLEDGMENTS AND DISCLOSURES

This research was supported by the National Natural Science Foundation of China (Grant Nos. 82001432 [to XY] and 81671344 [to XHM]), China Postdoctoral Science Foundation (Grant Nos. 2020TQ0213 and 2020M683319 [to XY]), Special Foundation for Brain Research from Science and Technology Program of Guangdong (Grant No. 2018B030334001 [to TL]), and the China Scholarship Council (Grant No. 201706240074 [to XY]).

The source data that support the findings in this report are available upon reasonable request to the corresponding author, and the supplementary information containing our structural covariance maps from MELODIC analysis and the corresponding subject loadings are available at the OSF link. In addition, the clustering algorithm is also publicly available. All these are available at https://osf.io/gnzsp/.

Over the past 3 years, DAP has received consulting fees from BlackThorn Therapeutics, Boehringer Ingelheim, Compass Pathway, Concert Pharmaceuticals, Engrail Therapeutics, Otsuka Pharmaceuticals, and Takeda Pharmaceuticals; one honorarium from Alkermes; and stock options from BlackThorn Therapeutics for activities unrelated to the current review. No funding from these entities was used to support the current work, and all views expressed are solely those of the authors. All other authors report no biomedical financial interests or potential conflicts of interest.

ARTICLE INFORMATION

From the Psychiatric Laboratory and Mental Health Center (XY, YD, MW, YC, TL, XM), the State Key Laboratory of Biotherapy, and Huaxi Brain Research Center (XY, YD, MW, YC, TL, XM), West China Hospital of Sichuan University, Chengdu, Sichuan, China; Center for Depression, Anxiety, and Stress Research (XY, PK, DAP), McLean Hospital, Belmont, Massachusetts; and Department of Psychiatry (PK, LDN, DAP) and McLean Imaging Center (LDN, DAP), McLean Hospital, Harvard Medical School, Boston, Massachusetts.

XY and PK contributed equally to this work as joint first authors.

DAP and XM contributed equally to this work as joint senior authors.

Address correspondence to Xiaohong Ma, M.D., at maxiaohong@scu.edu.cn.

Received Dec 8, 2020; revised Apr 20, 2021; accepted Apr 21, 2021.

Supplementary material cited in this article is available online at https://doi.org/10.1016/j.bpsgos.2021.04.006.

REFERENCES

1. Fried EI, Nesse RM (2015): Depression is not a consistent syndrome: An investigation of unique symptom patterns in the STAR*D study. J Affect Disord 172:96–102.
2. Beijers L, Wardenaar KJ, van Loo HM, Schoevers RA (2019): Data-driven biological subtypes of depression: Systematic review of biological approaches to depression subtyping. Mol Psychiatry 24:888–900.
3. Marquand AF, Wolfers T, Mennes M, Buitelaar J, Beckmann CF (2016): Beyond lumping and splitting: A review of computational approaches for stratifying psychiatric disorders. Biol Psychiatry Cogn Neurosci Neuroimaging 1:433–447.
4. van Loo HM, de Jonge P, Romeijn JW, Kessler RC, Schoevers RA (2012): Data-driven subtypes of major depressive disorder: A systematic review. BMC Med 10:156.
5. Drysdale AT, Grosenick L, Downar J, Dunlop K, Mansouri F, Meng Y, *et al.* (2017): Erratum: Resting-state connectivity biomarkers define neurophysiological subtypes of depression. Nat Med 23:264.
6. Price RB, Lane S, Gates K, Kraynak TE, Horner MS, Thase ME, Siegle GJ (2017): Parsing heterogeneity in the brain connectivity of

depressed and healthy adults during positive mood. Biol Psychiatry 81:347–357.
7. Yao D, Sui J, Wang M, Yang E, Jiaerken Y, Luo N, *et al.* (2021): A mutual multi-scale triplet graph convolutional network for classification of brain disorders using functional or structural connectivity. IEEE Trans Med Imaging 40:1279–1289.
8. Qi S, Schumann G, Bustillo J, Turner JA, Jiang R, Zhi D, *et al.* (2021): Reward processing in novelty seekers: A transdiagnostic psychiatric imaging biomarker [published online ahead of print Jan 30]. Biol Psychiatry.
9. Xu L, Groth KM, Pearlson G, Schretlen DJ, Calhoun VD (2009): Source-based morphometry: The use of independent component analysis to identify gray matter differences with application to schizophrenia. Hum Brain Mapp 30:711–724.
10. Nguyen L, Kakeda S, Watanabe K, Katsuki A, Sugimoto K, Igata N, *et al.* (2020): Brain structural network alterations related to serum cortisol levels in drug-naïve, first-episode major depressive disorder patients: A source-based morphometric study. Sci Rep 10:22096.
11. Hafkemeijer A, Altmann-Schneider I, de Craen AJ, Slagboom PE, van der Grond J, Rombouts SA (2014): Associations between age and gray matter volume in anatomical brain networks in middle-aged to older adults. Aging Cell 13:1068–1074.
12. Wang T, Wang K, Qu H, Zhou J, Li Q, Deng Z, *et al.* (2016): Disorganized cortical thickness covariance network in major depressive disorder implicated by aberrant hubs in large-scale networks. Sci Rep 6:27964.
13. Alexander-Bloch A, Raznahan A, Bullmore E, Giedd J (2013): The convergence of maturational change and structural covariance in human cortical networks. J Neurosci 33:2889–2899.
14. Evans AC (2013): Networks of anatomical covariance. NeuroImage 80:489–504.
15. He Y, Chen Z, Evans A (2008): Structural insights into aberrant topological patterns of large-scale cortical networks in Alzheimer's disease. J Neurosci 28:4756–4766.
16. Yao Z, Zhang Y, Lin L, Zhou Y, Xu C, Jiang T, Alzheimer's Disease Neuroimaging Initiative (2010): Abnormal cortical networks in mild cognitive impairment and Alzheimer's disease. PLoS Comput Biol 6: e1001006.
17. Beckmann CF, Smith SM (2005): Tensorial extensions of independent component analysis for multisubject FMRI analysis. Neuroimage 25:294–311.
18. Greicius MD, Krasnow B, Reiss AL, Menon V (2003): Functional connectivity in the resting brain: A network analysis of the default mode hypothesis. Proc Natl Acad Sci U S A 100:253–258.
19. Eckert MA, Keren NI, Roberts DR, Calhoun VD, Harris KC (2010): Age-related changes in processing speed: Unique contributions of cerebellar and prefrontal cortex. Front Hum Neurosci 4:10.
20. Beckmann CF, DeLuca M, Devlin JT, Smith SM (2005): Investigations into resting-state connectivity using independent component analysis. Philos Trans R Soc Lond B Biol Sci 360:1001–1013.
21. Damoiseaux JS, Rombouts SA, Barkhof F, Scheltens P, Stam CJ, Smith SM, Beckmann CF (2006): Consistent resting-state networks across healthy subjects. Proc Natl Acad Sci U S A 103:13848–13853.
22. Habas C, Kamdar N, Nguyen D, Prater K, Beckmann CF, Menon V, Greicius MD (2009): Distinct cerebellar contributions to intrinsic connectivity networks. J Neurosci 29:8586–8594.
23. Eckert MA, Leonard CM, Richards TL, Aylward EH, Thomson J, Berninger VW (2003): Anatomical correlates of dyslexia: Frontal and cerebellar findings. Brain 126:482–494.
24. Honey CJ, Kötter R, Breakspear M, Sporns O (2007): Network structure of cerebral cortex shapes functional connectivity on multiple time scales. Proc Natl Acad Sci U S A 104:10240–10245.
25. Wu H, Sun H, Wang C, Yu L, Li Y, Peng H, *et al.* (2017): Abnormalities in the structural covariance of emotion regulation networks in major depressive disorder. J Psychiatr Res 84:237–242.
26. First MB, Spitzer RL, Gibbon M, Williams JBW (1997): User's Guide for the Structured Clinical Interview for DSM-IV Axis I Disorders SCID-I: Clinician Version. Washington, DC: American Psychiatric Press.
27. Hamilton M (1960): A rating scale for depression. J Neurol Neurosurg Psychiatry 23:56–62.
28. Gong Y (1992): Wechsler Adult Intelligence Scale-Revised in China Version. Changsha: Hunan Medical College.
29. Douaud G, Smith S, Jenkinson M, Behrens T, Johansen-Berg H, Vickers J, *et al.* (2007): Anatomically related grey and white matter abnormalities in adolescent-onset schizophrenia. Brain 130:2375–2386.
30. Aad G, Abbott B, Abdallah J, Abdelalim AA, Abdesselam A, Abdinov O, *et al.* (2012): Determination of the strange-quark density of the proton from ATLAS measurements of the $W \to \ell\nu$ and $Z \to \ell\ell$ cross sections. Phys Rev Lett 109:012001.
31. Smith SM, Jenkinson M, Woolrich MW, Beckmann CF, Behrens TE, Johansen-Berg H, *et al.* (2004): Advances in functional and structural MR image analysis and implementation as FSL. Neuroimage 23(suppl 1):S208–S219.
32. Andersson JLR, Jenkinson M, Smith S (2007): Non-Linear Registration, aka Spatial Normalisation. FMRIB Technical Report TR07JA2. Oxford: FMRIB Centre.
33. Good CD, Johnsrude IS, Ashburner J, Henson RN, Friston KJ, Frackowiak RS (2001): A voxel-based morphometric study of ageing in 465 normal adult human brains. Neuroimage 14:21–36.
34. Smith SM, Fox PT, Miller KL, Glahn DC, Fox PM, Mackay CE, *et al.* (2009): Correspondence of the brain's functional architecture during activation and rest. Proc Natl Acad Sci U S A 106:13040–13045.
35. Laird AR, Fox PM, Eickhoff SB, Turner JA, Ray KL, McKay DR, *et al.* (2011): Behavioral interpretations of intrinsic connectivity networks. J Cogn Neurosci 23:4022–4037.
36. Qi S, Yang X, Zhao L, Calhoun VD, Perrone-Bizzozero N, Liu S, *et al.* (2018): MicroRNA132 associated multimodal neuroimaging patterns in unmedicated major depressive disorder. Brain 141:916–926.
37. Guo X, Wang Y, Guo T, Chen K, Zhang J, Li K, *et al.* (2015): Structural covariance networks across healthy young adults and their consistency. J Magn Reson Imaging 42:261–268.
38. Gupta CN, Turner JA, Calhoun VD (2019): Source-based morphometry: A decade of covarying structural brain patterns. Brain Struct Funct 224:3031–3044.
39. Segall JM, Allen EA, Jung RE, Erhardt EB, Arja SK, Kiehl K, Calhoun VD (2012): Correspondence between structure and function in the human brain at rest. Front Neuroinform 6:10.
40. Gong Q, He Y (2015): Depression, neuroimaging and connectomics: A selective overview. Biol Psychiatry 77:223–235.
41. Kaiser RH, Andrews-Hanna JR, Wager TD, Pizzagalli DA (2015): Large-scale network dysfunction in major depressive disorder: A meta-analysis of resting-state functional connectivity. JAMA Psychiatry 72:603–611.
42. MacQueen J (1967): Some methods for classification and analysis of multivariate observations. In: Le Cam LM, Neyman J, editors. Proceedings of the Fifth Berkeley Symposium on Mathematical Statistics and Probability, vol. 1: Theory of Statistics. Berkeley: University of California Press, 281–297.
43. Rousseeuw PJ (1987): Silhouettes: A graphical aid to the interpretation and validation of cluster analysis. J Comp Appl Math 20:53–65.
44. Caliński T, Harabasz J (1974): A dendrite method for cluster analysis. Commun Stat 3:1–27.
45. Tibshirani R, Walther G, Hastie T (2001): Estimating the number of clusters in a data set via the gap statistic. J R Stat Soc B 63:411–423.
46. Davies DL, Bouldin DW (1979): A cluster separation measure. IEEE Trans Pattern Anal Mach Intell 1:224–227.
47. Alexander-Bloch A, Giedd JN, Bullmore E (2013): Imaging structural co-variance between human brain regions. Nat Rev Neurosci 14:322–336.
48. Wright IC, Sharma T, Ellison ZR, McGuire PK, Friston KJ, Brammer MJ, *et al.* (1999): Supra-regional brain systems and the neuropathology of schizophrenia. Cereb Cortex 9:366–378.
49. Rockel AJ, Hiorns RW, Powell TP (1980): The basic uniformity in structure of the neocortex. Brain 103:221–244.

50. Lerch JP, Worsley K, Shaw WP, Greenstein DK, Lenroot RK, Giedd J, Evans AC (2006): Mapping anatomical correlations across cerebral cortex (MACACC) using cortical thickness from MRI. Neuroimage 31:993–1003.
51. Gong G, Rosa-Neto P, Carbonell F, Chen ZJ, He Y, Evans AC (2009): Age- and gender-related differences in the cortical anatomical network. J Neurosci 29:15684–15693.
52. Liao W, Zhang Z, Mantini D, Xu Q, Wang Z, Chen G, *et al.* (2013): Relationship between large-scale functional and structural covariance networks in idiopathic generalized epilepsy. Brain Connect 3:240–254.
53. Menon V (2011): Large-scale brain networks and psychopathology: A unifying triple network model. Trends Cogn Sci 15:483–506.
54. Hafkemeijer A, Möller C, Dopper EG, Jiskoot LC, van den Berg-Huysmans AA, van Swieten JC, *et al.* (2016): Differences in structural covariance brain networks between behavioral variant frontotemporal dementia and Alzheimer's disease. Hum Brain Mapp 37:978–988.
55. Seeley WW, Crawford RK, Zhou J, Miller BL, Greicius MD (2009): Neurodegenerative diseases target large-scale human brain networks. Neuron 62:42–52.
56. Scheinost D, Holmes SE, DellaGioia N, Schleifer C, Matuskey D, Abdallah CG, *et al.* (2018): Multimodal investigation of network level effects using intrinsic functional connectivity, anatomical covariance, and structure-to-function correlations in unmedicated major depressive disorder. Neuropsychopharmacology 43:1119–1127.
57. Drysdale AT, Grosenick L, Downar J, Dunlop K, Mansouri F, Meng Y, *et al.* (2017): Resting-state connectivity biomarkers define neurophysiological subtypes of depression. Nat Med 23:28–38.
58. Zheng H, Xu L, Xie F, Guo X, Zhang J, Yao L, Wu X (2015): The altered triple networks interaction in depression under resting state based on graph theory. Biomed Res Int 2015:386326.
59. Zhi D, Calhoun VD, Lv L, Ma X, Ke Q, Fu Z, *et al.* (2018): Aberrant dynamic functional network connectivity and graph properties in major depressive disorder. Front Psychiatry 9:339.
60. Fox MD, Snyder AZ, Vincent JL, Corbetta M, Van Essen DC, Raichle ME (2005): The human brain is intrinsically organized into dynamic, anticorrelated functional networks. Proc Natl Acad Sci U S A 102:9673–9678.
61. Hamilton JP, Farmer M, Fogelman P, Gotlib IH (2015): Depressive rumination, the default-mode network, and the dark matter of clinical neuroscience. Biol Psychiatry 78:224–230.
62. Burkhouse KL, Jacobs RH, Peters AT, Ajilore O, Watkins ER, Langenecker SA (2017): Neural correlates of rumination in adolescents with remitted major depressive disorder and healthy controls. Cogn Affect Behav Neurosci 17:394–405.
63. Hamilton JP, Furman DJ, Chang C, Thomason ME, Dennis E, Gotlib IH (2011): Default-mode and task-positive network activity in major depressive disorder: Implications for adaptive and maladaptive rumination. Biol Psychiatry 70:327–333.
64. Greicius MD, Flores BH, Menon V, Glover GH, Solvason HB, Kenna H, *et al.* (2007): Resting-state functional connectivity in major depression: Abnormally increased contributions from subgenual cingulate cortex and thalamus. Biol Psychiatry 62:429–437.
65. Drevets WC, Ongür D, Price JL (1998): Neuroimaging abnormalities in the subgenual prefrontal cortex: Implications for the pathophysiology of familial mood disorders. Mol Psychiatry 3:220-226, 190–191.
66. Seeley WW, Menon V, Schatzberg AF, Keller J, Glover GH, Kenna H, *et al.* (2007): Dissociable intrinsic connectivity networks for salience processing and executive control. J Neurosci 27:2349–2356.
67. Drevets WC (2007): Orbitofrontal cortex function and structure in depression. Ann N Y Acad Sci 1121:499–527.
68. Schmitt JE, Eyler LT, Giedd JN, Kremen WS, Kendler KS, Neale MC (2007): Review of twin and family studies on neuroanatomic phenotypes and typical neurodevelopment. Twin Res Hum Genet 10:683–694.
69. Bernhardt BC, Chen Z, He Y, Evans AC, Bernasconi N (2011): Graph-theoretical analysis reveals disrupted small-world organization of cortical thickness correlation networks in temporal lobe epilepsy. Cereb Cortex 21:2147–2157.
70. Chen CH, Gutierrez ED, Thompson W, Panizzon MS, Jernigan TL, Eyler LT, *et al.* (2012): Hierarchical genetic organization of human cortical surface area. Science 335:1634–1636.
71. Abas MA, Sahakian BJ, Levy R (1990): Neuropsychological deficits and CT scan changes in elderly depressives. Psychol Med 20:507–520.
72. Afridi MI, Hina M, Qureshi IS, Hussain M (2011): Cognitive disturbance comparison among drug-naive depressed cases and healthy controls. J Coll Physicians Surg Pak 21:351–355.
73. Gold JM, Goldberg RW, McNary SW, Dixon LB, Lehman AF (2002): Cognitive correlates of job tenure among patients with severe mental illness. Am J Psychiatry 159:1395–1402.
74. Etkin A, Patenaude B, Song YJ, Usherwood T, Rekshan W, Schatzberg AF, *et al.* (2015): A cognitive-emotional biomarker for predicting remission with antidepressant medications: A report from the iSPOT-D trial. Neuropsychopharmacology 40:1332–1342.
75. Yang X, Ma X, Huang B, Sun G, Zhao L, Lin D, *et al.* (2015): Gray matter volume abnormalities were associated with sustained attention in unmedicated major depression. Compr Psychiatry 63:71–79.
76. Lin K, Xu G, Lu W, Ouyang H, Dang Y, Lorenzo-Seva U, *et al.* (2014): Neuropsychological performance in melancholic, atypical and undifferentiated major depression during depressed and remitted states: A prospective longitudinal study. J Affect Disord 168:184–191.
77. Bortolato B, Miskowiak KW, Köhler CA, Maes M, Fernandes BS, Berk M, Carvalho AF (2016): Cognitive remission: A novel objective for the treatment of major depression? BMC Med 14:9.
78. Klein DN (2008): Classification of depressive disorders in the DSM-V: Proposal for a two-dimension system. J Abnorm Psychol 117:552–560.
79. Weinberg A, Perlman G, Kotov R, Hajcak G (2016): Depression and reduced neural response to emotional images: Distinction from anxiety, and importance of symptom dimensions and age of onset. J Abnorm Psychol 125:26–39.